

Interestingly, some studies did not find changes in CH and CRF despite an iatrogenic change in corneal biomechanics caused by collagen crosslinking.⁷⁻⁹

The signal of the biomechanical waveform analysis device provides a morphologically unique fingerprint for each eye and may contain valuable clinical information.¹⁰ The new software (version 2) allows more detailed analysis of the corneal deformation signal waveform by providing 37 parameters, each of which describes a morphologic feature of the waveform. It is well established that the CH and CRF parameters are lower in keratoconic corneas and in those that have had laser in situ keratomileusis (LASIK) than in corneas that have not had surgery.^{2,11} Despite this difference, it is clinically apparent that most post-myopic LASIK corneas are not at risk for developing ectasia and, therefore, have a biomechanical profile that differs significantly from keratoconus.^{2,11}

In this study, we compared the biomechanical properties of keratoconic and post-femtosecond LASIK patients using corneal deformation signal waveform analysis in an attempt to quantify these differences and to assess the ability of these parameters to distinguish between these 2 groups (Figure 1). To our knowledge, this is the first study that examines differences in the biomechanical properties of keratoconic and post-femtosecond LASIK patients using corneal deformation signal waveform analysis.

PATIENTS AND METHODS

This retrospective chart review study was performed at the UCLA Laser Refractive Center, Jules Stein Eye Institute, University of California, Los Angeles. Data from patients with manifest keratoconus and post-femtosecond LASIK

Submitted: June 17, 2011.

Final revision submitted: November 4, 2011.

Accepted: November 11, 2011.

From Jules Stein Eye Institute, University of California, Los Angeles, California, USA.

Dr. Zarei-Ghanavati is the recipient of the 2010 International Council of Ophthalmology-Helmerich fellowship award and has received funding from ICO and Mashhad University of Medical Sciences, Mashhad, Iran. Dr. Ramirez-Miranda is the recipient of 2011 Gillingham Pan-American Ophthalmological Foundation fellowship award and has received funding from Conde de Valenciana Foundation, Mexico City, Mexico.

Presented at the annual meeting of the Association for Vision and Research in Ophthalmology, Fort Lauderdale, Florida, USA, May 2011.

Corresponding author: D. Rex Hamilton, MD, MS, Cornea and Uveitis Division, Jules Stein Eye Institute-UCLA, 100 Stein Plaza, Los Angeles, California 90095, USA. E-mail: hamilton@jsei.ucla.edu.

who presented in clinic between April 2005 and November 2010 were evaluated. Institutional review board approval was obtained, and the study followed the tenets of the Declaration of Helsinki.

Patients diagnosed with manifest keratoconus using clinical evaluation (scissoring of the retinoscopic reflex, slitlamp findings including Fleischer ring, Vogt striae, and prominent cornea nerves), topographic (OPD Scan, Nidek Co., Ltd.), and tomographic analysis (Orbscan II, Bausch & Lomb) were included in the study.

All post-femtosecond LASIK eyes included in the study had cleared the myopic LASIK preoperative screening process, including comprehensive ocular examination, topography, ultrasound pachymetry, tomography (Orbscan II), aberrometry (Ladarwave, Alcon Laboratories, Inc.), and biomechanical evaluation (Ocular Response Analyzer). All diagnoses and surgeries were performed by the same experienced cornea and refractive surgeon (D.R.H.). All eyes with previous ocular surgery, corneal scarring, a history of other ocular disease, or postoperative complications (in post-femtosecond LASIK group) were excluded. Post-femtosecond LASIK patients had been followed for at least 1 year to reduce the chance of including an eye with post-LASIK keratectasia in the normal post-femtosecond LASIK group.

Central corneal thickness (CCT) was obtained by ultrasonic pachymetry (Tomey SP-3000, Tomey, Ltd.) in both groups. Flap thickness was calculated by subtracting the stromal bed thickness measured intraoperatively after femtosecond-created flap lifting from preoperative CCT.

The Ocular Response Analyzer with software version 2.04 was used to obtain the CH, CRF, and 37 corneal deformation signal waveform parameters. These parameters describe various mathematic features of the corneal deformation signal, and their description is shown in Table 1. Figure 2 shows the location of some of the parameters on a representative corneal deformation signal waveform. The measurements were taken at least 3 times, and the measurement with the highest waveform score was used. The waveform score is a composite index based on 5 mathematic aspects of the corneal deformation signal. The score ranges from 0 to 10, with a higher score indicating that the signal is closer to an ideal signal from a normal cornea.

Statistical analysis was performed using SAS software (version 9.1, SAS Institute, Inc.). Univariate (*t* test and Fisher exact test) and multivariable regression models were used to compare variables between groups. To address the potential confounding effect of CCT and age, a multivariate logistic regression model was used to control for these parameters. After controlling for CCT and age, a multivariate logistic regression model with stepwise variable selection method was used to select the parameters that were most useful in distinguishing between the keratoconic group and the post-femtosecond LASIK group. The area under a receiver operating characteristic (ROC) curve for this function was also calculated. A *P* value less than 0.05 was considered statistically significant.

RESULTS

Ninety-four post-femtosecond LASIK eyes of 51 patients and 105 eyes of 76 patients with manifest keratoconus were included in the study. Table 2 shows the demographics of the study groups. There were statistically significantly more men than women in

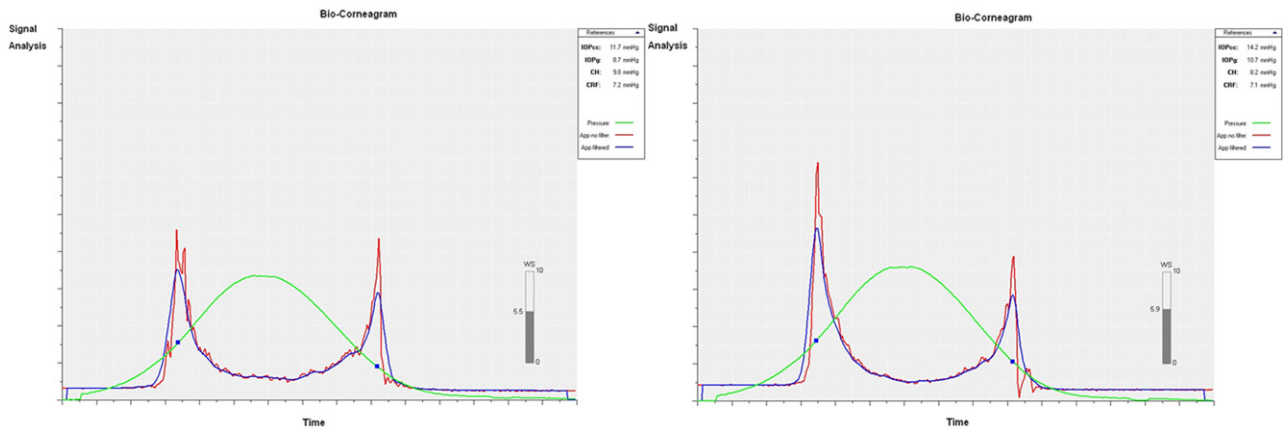


Figure 1. The waveform in a keratoconic cornea (*right*) and a post-femtosecond LASIK cornea (*left*). Gross comparison shows differences in both peaks including the slopes and the noise (App = applanation; CH = corneal hysteresis; CRF = corneal resistance factor; IOPcc = corneal-compensated intraocular pressure; IOPg = Goldmann-correlated intraocular pressure).

the keratoconus group. There were no statistically significant differences in age or race between the groups ($P = .33$ and $P = 1.00$, respectively).

Preoperative refractive error in the post-femtosecond LASIK group was -3.82 ± 1.69 diopters (D) (range -1.00 to -9.50). At follow-up, the mean refractive error was 0.14 ± 0.40 D (range -2.00 to $+1.00$ D). The mean flap thickness in post-femtosecond LASIK was 119.4 ± 11.5 μm (range 97.0 to 143.0 μm). The mean CCT in the post-femtosecond LASIK and keratoconus groups was 478.5 ± 28.9 μm (range 392.3 to 539.3 μm) and 454.8 ± 51.1 μm (range 370.0 to 461.9 μm), respectively ($P = .0001$).

Table 3 shows univariate analysis of the various parameters between the 2 groups. The differences in CH and CRF were statistically significant between the groups ($P < .0001$ and $P = .006$, respectively). There was no significant between-group difference between in the peak heights of the 2 peaks of the corneal deformation signal waveform (P1 and P2, respectively).

After statistically controlling for differences in CCT and age using a multivariate logistic regression model with stepwise variable selection, the CRF mean difference was not statistically significant; however, differences between the means of CH ($P = .035$) and 6 waveform parameters were statistically significant (Table 4). The area under the ROC curve for this model using CH and the 6 corneal deformation signal waveform parameters was 0.932 (Figure 3). For this logistic regression model, at the best cutoff point, the sensitivity was 81.0%, the specificity was 85.1%, and overall accuracy was 82.9%.

DISCUSSION

This study was designed to compare the corneal biomechanical waveforms between post-femtosecond

LASIK and keratoconic eyes by analyzing CH, CRF, P1, P2, and 37 corneal deformation signal waveform parameters. There are several studies in the literature analyzing aspects of the Ocular Response Analyzer corneal deformation signal waveform other than CH and CRF.^{12,13} The clinical significance of these various waveform parameters is currently unknown. The purpose of our study was to identify which of the new parameters could differentiate post-femtosecond LASIK corneas from those with manifest keratoconus after controlling for potential confounding factors such as CCT and age.

Bowman layer and the corneal stroma are thought to provide the majority of the biomechanical strength, although the role of Bowman layer has been a subject of controversy.¹⁴

Keratoconus is an asymmetric bilateral noninflammatory thinning of the corneal stroma. It is characterized by irregular astigmatism and asymmetric corneal thinning. Histopathological studies¹⁵⁻¹⁷ show breaks in Bowman layer, collagen bundle separation, and a decrease in the number of collagen fibers.

In contrast, the LASIK procedure involves cutting a stromal flap and ablating the underlying stromal bed of a normal cornea. In this study, we excluded from our study eyes that had LASIK using a microkeratome to reduce the confounding effect of flap-induced biomechanical variability.^{18,19} We evaluated whether the Ocular Response Analyzer device provides information to distinguish biomechanical differences between a pathologic disease (keratoconus) and an iatrogenically altered normal cornea (post-femtosecond flap LASIK).

Several studies have shown that myopic LASIK causes a general reduction in CH and CRF.^{2,5,6} It has also been reported that changes in CH and CRF after femtosecond LASIK strongly correlate with ablation

Table 1. Description of optical corneal deformation signal parameters.

Parameter	Name	Description
1	aindex	Degree of “non-monotonicity” of rising and falling edges of peak1 (normalized by area)
2	bindex	Degree of “non-monotonicity” of rising and falling edges of peak2 (normalized by area)
3	p1area	Area of peak1 (sum of values)
4	p2area	Area of peak2 (sum of values)
5	aspect1	Aspect ratio of peak1 (height/width)
6	aspect2	Aspect ratio of peak2 (height/width)
7	uslope1	Upslope of peak1 (base to peak value of peak1)
8	uslope2	Upslope of peak2 (base to peak value of peak2) (downslope in real time of peak2)
9	dslope1	Downslope of peak1 (base to peak value of peak1)
10	dslope2	Downslope of peak2 (base to peak value of peak2) (upslope in real time of peak2)
11	w1	Width of peak1 at base of peak1 region
12	w2	Width of peak2 at base of peak2 region
13	h1	Height of peak1 (from lowest to highest value in peak1 region)
14	h2	Height of peak2 (from lowest to highest value in peak2 region)
15	dive1	Absolute value of monotonic decrease on downslope part of peak1 starting at the peak value
16	dive2	Absolute value of monotonic decrease on downslope part of peak2 starting at the peak value (montonic increase in real time for peak2)
17	path1	Absolute value of path length around peak1
18	path2	Absolute value of path length around peak2
19	mslew1	Maximum single step increase in rise of peak1
20	mslew2	Maximum single step increase in rise of peak2
21	slew1	Aspect ratio of dive1 (value of dive divided by width of dive region)
22	slew2	Aspect ratio of dive2 (value of dive divided by width of dive region)
23	aplfh	High-frequency noise in region between peaks (normalized by product of average of peak heights times width of region)
24	p1area1	Area of peak1 (sum of values)
25	p2area1	Area of peak2 (sum of values)
26	aspect11	Aspect ratio of peak1 (height/width)
27	aspect21	Aspect ratio of peak2 (height/width)
28	uslope11	Upslope of peak1 (base to peak value of peak1)
29	uslope21	Upslope of peak2 (base to peak value of peak2) (downslope in real time of peak2)
30	dslope11	Downslope of peak1 (base to peak value of peak1)
31	dslope21	Downslope of peak2 (base to peak value of peak2) (upslope in real time of peak2)
32	w11	Width of peak1 at base of peak1 region
33	w21	Width of peak2 at base of peak2 region
34	h11	Height of peak1 (from lowest to highest value in peak1 region)
35	h21	Height of peak2 (from lowest to highest value in peak2 region)
36	path11	Absolute value of path length around peak1
37	path21	Absolute value of path length around peak2

Notes: Parameters 1–24 are derived from upper 75% of applanation peak (defined on baseline-subtracted signal). The 2nd applanation region is time reversed so that the upslope (uslope notation) of peak2 is actually a downslope (dslope notation) in real time. Parameters 24–37 have same descriptions as parameters 3–14, 17, and 18 except they are derived from the upper 50% of the applanation peaks.

depth. This suggests that alteration in corneal biomechanics is associated with attempted correction.^{16,20}

Shah et al.¹¹ showed that keratoconic eyes have significantly lower CH than normal eyes. Other studies

showed that although both CH and CRF are significantly lower in keratoconic eyes, a large overlap exists between normal eyes and keratoconic eyes.^{2,11} Shah and Laiquzzaman²¹ compared biomechanical

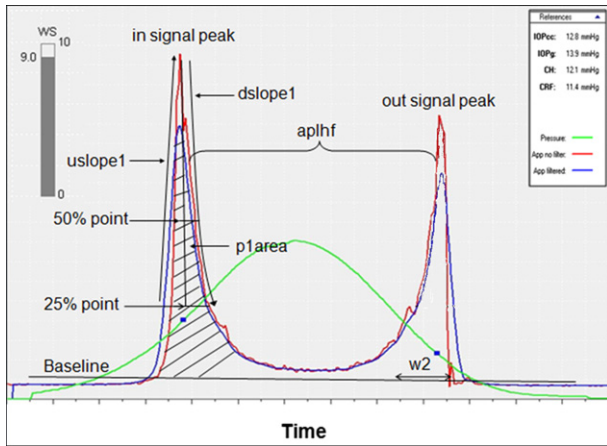


Figure 2. Corresponding location on corneal deformation signal waveform for parameters with statistically significant difference between manifest keratoconus and post-femtosecond LASIK groups. (See Figure 1 legend and Table 1 for a description of the parameters.)

parameters (CH and CRF) of post-LASIK and keratoconus and found very similar changes in both groups. In contrast, Ortiz et al.²² showed that CH and CRF values were significantly lower in keratoconic eyes than in post-LASIK eyes. Neither of the 2 studies controlled for potential confounding factors, such as CCT or age.

In our study, univariate analysis showed a lower mean CH in the keratoconus group. The CH is defined as the absolute difference between the peak pressure values causing inward and outward corneal

applanations (P1 – P2). It represents the viscoelastic property of the cornea. We also found a lower mean CRF in keratoconic patients under univariate analysis. The CRF is derived from the formula (P1 – kP2), where k is a constant that is strongly associated with CCT. This renders CRF more CCT-dependent than CH.^{1,23-25} The CRF is usually considered to be the parameter most closely related to corneal elasticity.^{1,26,27} In a clinical study, Touboul et al.¹³ confirmed this and found a strong positive correlation between CRF and CCT and a low correlation for CH.

We tried to control for potential confounding factors using multivariate analysis. The mean CCT was 24 μm thicker in post-femtosecond LASIK eyes. Although the significance of this difference with regard to biomechanics is unknown, it is reasonable to assume there may be a correlation between biomechanical strength and CCT. As a consequence, we controlled for CCT as a confounding factor in multivariate analysis. Aging changes both CH and CRF.^{28,29} Therefore, age should be considered a confounding factor in studies of corneal biomechanics. In our study, there was no statistically significant difference in age between the 2 groups. Nevertheless, we adjusted for age in the multivariate analysis.

Multivariate analysis showed that after controlling for CCT and age, the difference in CH was still statistically significant between the 2 groups while the difference in CRF was no longer significant. The loss of significance of the CRF difference may relate to the parameter’s correlation with CCT.²⁷

In this study, multivariate logistic regression model analysis that controlled for potential confounding factors found that CH ($P=.003$) and 6 corneal deformation signal waveform parameters (P1area, $P=.042$; uslope1, $P=.0007$; dslop1, $P=.0001$; w2, $P=.003$; aindex, $P=.0004$); and aplhf, $P<.0001$) had the best statistical ability to differentiate between post-LASIK corneas and keratoconic corneas. How these parameters represent biomechanical properties of the cornea is still unknown and should be a focus of future studies. Keratoconus and myopic LASIK cause opposing changes in corneal curvature. Keratoconic corneas are steeper and post-myopic LASIK corneas are flatter than normal unaltered corneas. Although several studies^{10,23,30,31} showed no correlation between the main Ocular Response Analyzer parameters (CH, CRF) and corneal curvature, there might be an association between curvature and certain corneal deformation signal waveform parameters. In general, the keratoconic cornea does not flatten as uniformly as a normal cornea. This likely leads to overall lower corneal deformation signal amplitudes and more noisy signals. For example, the time during which the maximum area of the cornea is flattened is

Table 2. Demographics by group.

Characteristic	Post-LASIK (n = 51)	Keratoconus (n = 76)	P Value
Age (y)			.33*
Mean ± SD	35.6 ± 9.2	37.6 ± 12.1	
Median	34.0	36.3	
Range	23.0, 56.0	17.1, 67.3	
Sex, n (%)			.001†
Male	24 (47)	58 (76)	
Female	27 (53)	18 (24)	
Race, n (%)			1.00‡
White	22 (61)	37 (61)	
African-American	3 (6)	6 (10)	
Hispanic	6 (17)	15 (25)	
Asian	5 (14)	3 (5)	
Unknown	15	15	

LASIK = femtosecond laser in situ keratomileusis

*t test for the difference between post-femtosecond LASIK and keratoconus groups

†Fisher exact test for the difference between post-femtosecond LASIK and keratoconus groups

‡Comparing white race with all other race categories combined

Table 3. Univariate comparison of CH, CRF, CCT, P1, P2 and 37 corneal deformation signal waveform parameters between groups.

Parameter*	Post-Femtosecond LASIK Group				Keratoconus Group				P Value
	Mean	SD	Lower Quartile	Upper Quartile	Mean	SD	Lower Quartile	Lower Quartile	
CCT (μ m)	478.5	28.9	458.0	497.2	454.8	51.1	421.0	493.0	.0001
CH (mm Hg)	9.2	1.2	8.4	10.0	8.2	1.5	7.1	9.1	<.0001
CRF (mm Hg)	8.2	1.5	7.1	9.1	7.5	1.8	6.3	8.4	.0006
P1	15.9	2.8	14.0	17.7	15.8	3.6	13.1	17.6	.74
P2	6.7	2.6	4.8	8.2	7.5	3.7	5.1	9.8	.075
aindex	9.1	1.2	8.7	10.0	7.8	2.0	6.6	9.2	<.0001
bindex	9.4	1.1	9.1	10.0	8.1	2.4	6.6	10.0	<.0001
p1area	2595.5	636.8	2216.0	2942.0	2578.5	1071.5	1708.6	3316.5	.89
p2area	1831.9	505.2	1417.0	2124.0	1680.3	692.6	1246.8	2089.9	.082
aspect1	15.1	5.8	11.0	18.6	15.8	8.5	9.5	20.8	.51
aspect2	20.0	8.4	13.5	25.7	15.0	9.3	8.0	20.7	.0001
uslope1	73.8	33.8	49.2	99.0	62.3	39.2	34.9	80.4	.028
uslope2	101.5	36.3	82.8	121.5	69.7	45.8	36.7	98.8	<.0001
dslope1	19.7	7.8	13.8	26.0	22.8	13.4	13.0	28.9	.057
dslope2	25.5	12.2	16.6	32.1	20.0	12.9	11.1	26.5	.002
w1	22.5	4.5	2.0	25.0	22.3	6.1	18.0	25.0	.77
w2	16.8	4.7	14.0	19.0	20.0	7.8	15.0	23.0	.0006
h1	316.8	81.0	267.9	373.9	316.7	133.1	223.7	413.1	1.00
h2	304.1	77.2	252.6	353.3	247.1	107.1	163.5	315.0	<.0001
dive1	274.8	94.1	211.3	340.5	265.0	134.2	174.8	354.5	.55
dive2	216.7	79.8	169.0	269.5	193.5	98.8	124.0	267.3	.072
path1	24.3	5.7	19.5	27.7	26.0	6.7	21.3	29.4	.062
path2	29.8	6.8	25.0	34.2	29.4	8.6	23.1	35.2	.70
mslew1	108.4	38.6	8.3	137.0	102.5	48.3	62.3	133.8	.34
mslew2	148.1	47.2	114.3	179.0	110.4	58.7	61.8	145.8	<.0001
slew1	74.2	33.6	49.4	99.0	64.6	38.7	37.5	87.1	.065
slew2	101.8	35.9	82.8	121.5	72.0	43.7	40.5	98.8	<.0001
aplhf	1.2	0.3	1.0	1.4	1.7	0.5	1.4	2.0	<.0001
p1area1	1019.1	306.1	832.3	1191.8	1038.8	483.0	727.8	1261.4	.74
p2area1	763.1	225.9	592.5	906.3	693.7	318.7	504.4	844.8	.082
aspect11	24.4	12.0	14.7	30.9	24.2	14.9	13.4	32.7	.92
aspect21	31.1	12.7	21.6	39.2	23.7	16.2	12.1	32.3	.0004
uslope11	68.2	32.1	41.3	90.3	61.8	38.2	33.2	83.4	.20
uslope21	81.3	35.4	55.8	103.5	58.9	38.3	29.8	78.0	<.0001
dslope11	38.5	22.5	23.4	51.8	42.4	30.6	21.1	57.2	.30
dslope21	49.1	25.3	31.4	63.1	38.6	28.7	17.6	53.9	.007
w11	10.1	3.5	8.0	12.0	10.4	3.7	8.0	12.0	.59
w21	7.2	2.4	6.0	8.0	8.8	3.9	6.0	11.0	.0007
h11	211.2	54.0	178.6	249.3	211.2	88.7	149.1	275.4	1.00
h21	202.8	51.5	168.4	235.5	164.7	71.4	109.0	210.0	<.0001
path11	37.1	10.0	29.6	42.6	37.7	10.3	30.5	43.8	.72
path21	43.0	12.7	34.4	49.6	40.8	13.0	30.6	49.9	.25

LASIK = laser in situ keratomileusis

*See Table 1 for description of parameters.

likely shorter in the keratoconic cornea than in the normal cornea. This may manifest as narrower corneal deformation signal peaks. Further studies may elucidate which quantifiable metrics from the corneal deformation signal waveform best describe the hallmarks of keratoconic corneal biomechanics.

Another possible confounding factor is post-LASIK dry eye. Dry eye is common after LASIK. It alters the tear breakup time and causes corneal surface irregularly.^{32,33} Because the corneal deformation signal is produced from light reflection from the cornea, any surface irregularity might change the reflected beam

Table 4. Waveform parameters that were statistically significantly different between the post-femtosecond LASIK group and the keratoconus group. Results are from a multivariate logistic regression model with stepwise variable selection after controlling of confounding factors.

Parameter*	OR [†]	95% CI	P Value
CH	0.68	0.47, 0.97	.035
p1area	1.11	1.03, 1.19	.006
upslop1	0.74	0.62, 0.89	.001
dslop1	1.18	1.09, 1.28	<.0001
w2	1.15	1.06, 1.26	.001
aindex	0.51	0.35, 0.75	.0007
aplhf	1.47	1.25, 1.73	<.0001

CI = confidence interval; OR = odds ratio

*See Table 1 for description of parameters.

[†]Odds ratio of keratoconus versus post-femtosecond LASIK. An odds ratio greater than 1 indicates that a keratoconus eye is more likely to have higher parameter values, while an odds ratio less than 1 indicates that a keratoconus eye is more likely to have lower parameter values

and alter the corneal deformation signal waveform parameters, especially those associated with signal quality, such as aplhf (high frequency noise in the region between P1 and P2).

In conclusion, we found statistically significant differences in the mean CH and 6 other waveform parameters between keratoconic corneas and post-femtosecond LASIK corneas after controlling for CCT and age. This study shows that analysis of the parameters derived from the corneal deformation signal waveform could improve our understanding of the differences between a pathologic condition such as keratoconus and a surgically altered normal cornea such as the post-LASIK condition. Further studies are needed to evaluate the biomechanical relevance and clinical importance of these new parameters.

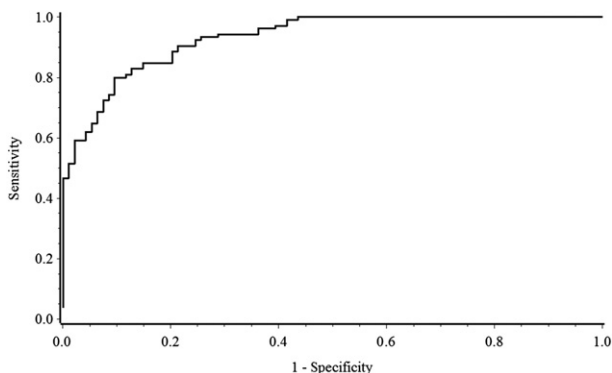


Figure 3. The area under the ROC curve for the model using corneal deformation signal parameters is 0.932.

REFERENCES

- Luce DA. Determining in vivo biomechanical properties of the cornea with an ocular response analyzer. *J Cataract Refract Surg* 2005; 31:156–162
- Ortiz D, Piñero D, Shabayek MH, Arnalich-Montiel F, Alió JL. Corneal biomechanical properties in normal, post-laser in situ keratomileusis, and keratoconic eyes. *J Cataract Refract Surg* 2007; 33:1371–1375
- del Buey MA, Cristóbal JA, Ascaso FJ, Lavilla L, Lanchares E. Biomechanical properties of the cornea in Fuchs' corneal dystrophy. *Invest Ophthalmol Vis Sci* 2009; 50:3199–3202. Available at: <http://www.iovs.org/content/50/7/3199.full.pdf>. Accessed December 4, 2011
- Kirwan C, O'Keefe M. Measurement of intraocular pressure in LASIK and LASEK patients using the Reichert Ocular Response Analyzer and Goldmann applanation tonometry. *J Refract Surg* 2008; 24:366–370
- Chen MC, Lee N, Bourla N, Hamilton DR. Corneal biomechanical measurements before and after laser in situ keratomileusis. *J Cataract Refract Surg* 2008; 34:1886–1891
- Qazi MA, Sanderson JP, Mahmoud AM, Yoon EY, Roberts CJ, Pepose JS. Postoperative changes in intraocular pressure and corneal biomechanical metrics; laser in situ keratomileusis versus laser-assisted subepithelial keratectomy. *J Cataract Refract Surg* 2009; 35:1774–1788
- Wollensak G, Spoerl E, Seiler T. Stress-strain measurements of human and porcine corneas after riboflavin-ultraviolet-A-induced cross-linking. *J Cataract Refract Surg* 2003; 29:1780–1785
- Sedaghat M, Naderi M, Zarei-Ghanavati M. Biomechanical parameters of the cornea after collagen crosslinking measured by waveform analysis. *J Cataract Refract Surg* 2010; 36:1728–1731
- Goldich Y, Barkana Y, Morad Y, Hartstein M, Avni I, Zadok D. Can we measure corneal biomechanical changes after collagen cross-linking in eyes with keratoconus?—a pilot study. *Cornea* 2009; 28:498–502
- Franco S, Lira M. Biomechanical properties of the cornea measured by the Ocular Response Analyzer and their association with intraocular pressure and the central corneal curvature. *Clin Exp Optom* 2009; 92:469–475. Available at: <http://onlinelibrary.wiley.com/doi/10.1111/j.1444-0938.2009.00414.x/pdf>. Accessed December 4, 2011
- Shah S, Laiquzzaman M, Bhojwani R, Mantry S, Cunliffe I. Assessment of the biomechanical properties of the cornea with the Ocular Response Analyzer in normal and keratoconic eyes. *Invest Ophthalmol Vis Sci* 2007; 48:3026–3031. Available at: <http://www.iovs.org/cgi/reprint/48/7/3026>. Accessed December 4, 2011
- Avetisov SE, Novikov IA, Bubnova IA, Antonov AA, Siplivyi VI. Determination of corneal elasticity coefficient using the ORA database. *J Refract Surg* 2010; 26:520–524
- Touboul D, Roberts C, Kérautret J, Garra C, Maurice-Tison S, Saubusse E, Colin J. Correlations between corneal hysteresis, intraocular pressure, and corneal central pachymetry. *J Cataract Refract Surg* 2008; 34:616–622
- Komai Y, Ushiki T. The three-dimensional organization of collagen fibrils in the human cornea and sclera. *Invest Ophthalmol Vis Sci* 1991; 32:2244–2258. Available at: <http://www.iovs.org/cgi/reprint/32/8/2244>. Accessed December 4, 2011
- Krachmer JH, Feder RS, Belin MW. Keratoconus and related noninflammatory corneal thinning disorders. *Surv Ophthalmol* 1984; 28:293–322
- Rabinowitz YS. Keratoconus. *Surv Ophthalmol* 1998; 42:297–319

17. Bron AJ. Keratoconus. *Cornea* 1988; 7:163–169
18. Rosa AM, Neto Murta J, Quadrado MJ, Tavares C, Lobo C, Van Velze R, Castanheira-Dinis A. Femtosecond laser versus mechanical microkeratomers for flap creation in laser in situ keratomileusis and effect of postoperative measurement interval on estimated femtosecond flap thickness. *J Cataract Refract Surg* 2009; 35:833–838
19. Kezirian GM, Stonecipher KG. Comparison of the IntraLase femtosecond laser and mechanical keratomers for laser in situ keratomileusis. *J Cataract Refract Surg* 2004; 30:804–811
20. Hamilton DR, Johnson RD, Lee N, Bourla N. Differences in the corneal biomechanical effects of surface ablation compared with laser in situ keratomileusis using a microkeratome or femtosecond laser. *J Cataract Refract Surg* 2008; 34:2049–2056
21. Shah S, Laiquzzaman M. Comparison of corneal biomechanics in pre and post-refractive surgery and keratoconic eyes by Ocular Response Analyser. *Cont Lens Anterior Eye* 2009; 32:129–132; quiz 151
22. Ortiz D, Alió JL, Piñero D. Measurement of corneal curvature change after mechanical laser in situ keratomileusis flap creation and femtosecond laser flap creation. *J Cataract Refract Surg* 2008; 34:238–242
23. Chang P-Y, Chang S-W, Wang J-Y. Assessment of corneal biomechanical properties and intraocular pressure with the Ocular Response Analyzer in childhood myopia. *Br J Ophthalmol* 2010; 94:877–881
24. Fontes BM, Ambrósio R Jr, Velarde GC, Nosé W. Ocular response analyzer measurements in keratoconus with normal central corneal thickness compared with matched normal control eyes. *J Refract Surg* 2011; 27:209–215
25. Detry-Morel M, Jamart J, Pourjavan S. Evaluation of corneal biomechanical properties with the Reichert Ocular Response Analyzer. *Eur J Ophthalmol* 2011; 21:138–148
26. Kotecha A, Elsheikh A, Roberts CR, Zhu H, Garway-Heath DF. Corneal thickness- and age-related biomechanical properties of the cornea measured with the Ocular Response Analyzer. *Invest Ophthalmol Vis Sci* 2006; 47:5337–5347. Available at: <http://www.iovs.org/cgi/reprint/47/12/5337>. Accessed December 4, 2011
27. Kotecha A. What biomechanical properties of the cornea are relevant for the clinician? *Surv Ophthalmol* 2007; 52(suppl 2):S109–S114
28. Kida T, Liu JHK, Weinreb RN. Effects of aging on corneal biomechanical properties and their impact on 24-hour measurement of intraocular pressure. *Am J Ophthalmol* 2008; 146:567–572
29. Kamiya K, Shimizu K, Ohmoto F. Effect of aging on corneal biomechanical parameters using the Ocular Response Analyzer. *J Refract Surg* 2009; 25:888–893
30. Oncel B, Dinc UA, Gorgun E, Yalvaç BI. Diurnal variation of corneal biomechanics and intraocular pressure in normal subjects. *Eur J Ophthalmol* 2009; 19:798–803
31. Laiquzzaman M, Bhojwani R, Cunliffe I, Shah S. Diurnal variation of ocular hysteresis in normal subjects: relevance in clinical context. *Clin Exp Ophthalmol* 2006; 34:114–118
32. Yu EYW, Leung A, Rao S, Lam DSC. Effect of laser in situ keratomileusis on tear stability. *Ophthalmology* 2000; 107:2131–2135
33. Nettune GR, Pflugfelder SC. Post-LASIK tear dysfunction and dysesthesia. *Ocul Surf* 2010; 8:135–145



First author:

Siamak Zarei-Ghanavati, MD, FICO

*Jules Stein Eye Institute,
University of California,
Los Angeles, California, USA*